Heat capacities of dipolar fluids: ferromagnetic colloids

2008 J. Phys.: Condens. Matter 20 204112

(http://iopscience.iop.org/0953-8984/20/20/204112)

J. Phys.: Condens. Matter **20** (2008) 204112 (5pp) doi:10.1088/0953-8984/20/20/204112

Heat capacities of dipolar fluids: ferromagnetic colloids

Z Máté and I Szalai

Institute of Physics, University of Pannonia, H-8201 Veszprém, PO Box 158, Hungary

E-mail: matez@almos.vein.hu and szalai@almos.vein.hu

Received 1 April 2008
Published 1 May 2008
Online at stacks.iop.org/JPhysCM/20/204112

Abstract

The heat capacities of ferrofluids are investigated using a thermodynamic perturbation theory approach and the NVT and NpT Monte Carlo simulation methods. The systems studied are considered as one-, three-, and five-component dipolar mixtures modeled by the Stockmayer interaction potential. The isochoric and isobaric heat capacities are calculated and compared with the data determined for a monodisperse equivalent of the system.

1. Introduction

Magnetic fluids are stable colloidal dispersions of magnetic particles coated with ionic groups or polymer surfactants in liquid carriers. An inherent feature of real ferrocolloids is that the nanoparticles differ in size and magnetic moment. This polydispersity affects the equation of state of the system and may have important consequences for the phase behavior, in particular for the fluid–fluid coexistence [1, 2]. This property also affects the equilibrium magnetization for dense as well as for dilute liquids. Recently, the influence of realistic polydispersity on the equilibrium magnetization properties of model and real ferrofluids was investigated by means of simulation and theory, and it was found that the magnetization is generally higher in the polydisperse system than in the monodisperse equivalent [3, 4]. The influence of polydispersity on the heat capacity along the phase separation curves was also studied in [5]. This work showed that the isochoric heat capacity was rather insensitive to the composition variations along the phase equilibrium curves.

In this work, our main goal is to study the influence of polydispersity on the bulk phase isochoric and isobaric heat capacities of magnetic fluids. The role of heat capacities is essential in both applications and theoretical thermodynamics [6, 7]. On the one hand, they can be measured by calorimetric methods. On the other hand, certain thermodynamic functions can be calculated from them. It could be important to know these physical properties of ferrocolloids for the calculation of the heating effects of biocompatible ferrofluids in altering magnetic fields [8]. In this paper, the heat capacities of polydisperse ferrofluids are approximated by the corresponding properties of one-, three-, and five-component dipolar mixtures. The interaction potential between two dipolar particles is modeled by the Stockmayer (STM) potential, which is the sum of the Lennard-Jones (LJ) and the dipole–dipole interactions. Both Monte Carlo (MC) simulations and perturbation theoretical (PT) calculations are used to compare the monodisperse heat capacities with the polydisperse ones.

2. Basic potential model

We consider a c-component mixture of spherical particles of diameter σ_i carrying a magnetic dipole moment $\mathbf{m}_i$. The isotropic part of the interparticle pair potential between particles of components i and j is modeled by the LJ potential

$$w_{ij}^{\mathrm{LJ}}(r_{12}) = 4\epsilon\left[\left(\frac{\sigma_{ij}}{r_{12}}\right)^{12} - \left(\frac{\sigma_{ij}}{r_{12}}\right)^{6}\right], \tag{1}$$

where ϵ is the energy parameter and $\sigma_{ij} = (\sigma_i + \sigma_j)/2$. In addition, the magnetic dipolar interaction is described via point dipoles embedded at the centers of the spheres

$$w_{ij}^{\mathrm{dd}}(\mathbf{r}_{12}, \omega_1, \omega_2) = -\frac{m_i m_j}{r_{12}^3}\left[\frac{3(\widehat{\mathbf{m}}_1 \cdot \mathbf{r}_{12})(\widehat{\mathbf{m}}_2 \cdot \mathbf{r}_{12})}{r_{12}^2} - (\widehat{\mathbf{m}}_1 \cdot \widehat{\mathbf{m}}_2)\right], \tag{2}$$

where $\mathbf{r}_{12} = \mathbf{r}_1 - \mathbf{r}_2$ is the interparticle separation vector, from the center of particle 1 to that of particle 2. Particle 1 (2) of type i (j) is located at $\mathbf{r}_1$ ($\mathbf{r}_2$) and carries a dipole moment of strength m_i (m_j) with an orientation given by the unit vector $\widehat{\mathbf{m}}_1$ ($\widehat{\mathbf{m}}_2$) or by the space angle ω_1 (ω_2). Thus the STM pair potential is given by

$$w_{ij}^{\mathrm{STM}}(\mathbf{r}_{12}, \omega_1, \omega_2) = w_{ij}^{\mathrm{LJ}}(r_{12}) + w_{ij}^{\mathrm{dd}}(\mathbf{r}_{12}, \omega_1, \omega_2). \tag{3}$$

3. Perturbation theory

The thermodynamic PT of dipolar fluids is based on the Gubbins–Pople–Stell [9] division of the interparticle potential into a reference and a perturbation part. The reference potential is obtained as an unweighted average over the orientations of dipoles 1 and 2:

$$w_{ij}^{\mathrm{ref}}(r_{12}) = \langle w_{ij}^{\mathrm{STM}}(\mathbf{r}_{12}, \omega_1, \omega_2)\rangle_{\omega_1,\omega_2} = w_{ij}^{\mathrm{LJ}}(r_{12}), \quad (4)$$

while the perturbation part is the dipole–dipole interaction potential. According to this division the perturbation expansion of the free energy of the STM fluid about a LJ reference system is given as

$$F^{\mathrm{c}} = F_{\mathrm{LJ}}^{\mathrm{c}} + F_1 + F_2 + F_3 + \cdots, \quad (5)$$

where $F_{\mathrm{LJ}}^{\mathrm{c}}$ is the configurational free energy of the reference system, F_1 is the first-order perturbation term, and so on. The free energy of the LJ reference fluid is calculated from an equation of state proposed by Johnson *et al* [10]. F_1 vanishes because the angular integral in this term is zero. The second-order term can be expressed as

$$F_2 = -\frac{2\pi}{3} N\beta\rho \sum_{i=1}^{\mathrm{c}} \sum_{j=1}^{\mathrm{c}} x_i x_j m_i^2 m_j^2 \frac{I_{ij}^{\mathrm{dd}}(\beta, \rho, x_i, x_j)}{\sigma_{ij}^3}, \quad (6)$$

where $\rho = N/V$ is the particle number density, $\beta = 1/(k_{\mathrm{B}}T)$ is the inverse temperature, and $x_i = N_i/N$ is the number fraction of component i. The third-order PT term is

$$F_3 = \frac{1}{54} N\beta^2\rho^2 \times \sum_{i=1}^{\mathrm{c}} \sum_{j=1}^{\mathrm{c}} \sum_{k=1}^{\mathrm{c}} x_i x_j x_k m_i^2 m_j^2 m_k^2 \frac{K_{ijk}^{\mathrm{ddd}}(\beta, \rho, x_i, x_j, x_k)}{\sigma_{ij}\sigma_{jk}\sigma_{ik}}. \quad (7)$$

In these equations I_{ij}^{dd} and K_{ijk}^{ddd} are integrals over the two- and three-particle correlation functions ($g_{ij}^{\mathrm{LJ}}(r_{12})$ and $g_{ijk}^{\mathrm{LJ}}(r_{12}, r_{23}, r_{13})$) for the reference fluid. These integrals have only been calculated for one-component fluids, using MC and molecular dynamics results for the LJ reference system. The resulting values have been fitted to simple functions of reduced temperature and density and can be found in [11]. To improve the convergence in equation (5) for the dipolar terms the Padé approximant is used:

$$F_{\mathrm{c}} = F_{\mathrm{c}}^{\mathrm{LJ}} + \frac{F_2}{1 - F_3/F_2}. \quad (8)$$

The integrals I_{ij}^{dd} and K_{ijk}^{ddd} cannot be calculated for a many-component mixture since the numerical data for the corresponding correlation functions are missing. However, these integrals are related to the corresponding one-component fluid integrals by the van der Waals one-fluid theory. In our case it means that the following approximations are used:

$$I_{ij}^{\mathrm{dd}}(\beta, \rho, x_i, x_j) = I^{\mathrm{dd}}(\beta, \rho\sigma_x^3), \quad (9)$$

and

$$K_{ijk}^{\mathrm{ddd}}(\beta, \rho, x_i, x_j, x_k) = K^{\mathrm{ddd}}(\beta, \rho\sigma_x^3). \quad (10)$$

The integrals I^{ddd} and K^{ddd} are one-component fluid integrals [11] calculated at the reduced density $\rho\sigma_x^3$, using the average diameter

$$\sigma_x^3 = \sum_{i=1}^{\mathrm{c}} \sum_{j=1}^{\mathrm{c}} x_i x_j \sigma_{ij}^3. \quad (11)$$

Note that there are other ways to approximate these mixture integrals, for example using the so called conformal solution expansion [12], which cancel the coupling in equations (6) and (7) and therefore the application is easier.

4. Heat capacities

The configurational isochoric heat capacity is defined as

$$C_V^{\mathrm{c}} = C_V - C_V^{\mathrm{id}} = \left(\frac{\partial U^{\mathrm{c}}}{\partial T}\right)_V = -T\left(\frac{\partial^2 F^{\mathrm{c}}}{\partial T^2}\right)_V, \quad (12)$$

where C_V is the total isochoric heat capacity, C_V^{id} is the ideal gas isochoric heat capacity, and U^{c} is the configurational internal energy. The corresponding equations for the isobaric heat capacity are

$$C_p^{\mathrm{c}} = C_p - C_p^{\mathrm{id}} + Nk_{\mathrm{B}} = C_p - C_V^{\mathrm{id}} = \left(\frac{\partial H^{\mathrm{c}}}{\partial T}\right)_p = -T\left(\frac{\partial^2 G^{\mathrm{c}}}{\partial T^2}\right)_p, \quad (13)$$

where C_p^{id} is the ideal gas isobaric heat capacity, H^{c} is the configurational enthalpy, and G^{c} is the configurational free enthalpy of the system. Here, the configurational isochoric heat capacity is calculated from equation (12), while for the calculation of C_p^{c} the following thermodynamic relation is applied:

$$C_p^{\mathrm{c}} = C_V^{\mathrm{c}} - T\left(\frac{\partial p}{\partial T}\right)_v^2 \left(\frac{\partial p}{\partial V}\right)_T^{-1}, \quad (14)$$

where p is the pressure of the system calculated from the free energy. The derivatives of thermodynamic functions can be calculated from fluctuation formulas in various ensembles. For example, in the NVT ensemble the isochoric heat capacity can be obtained as

$$C_v = \frac{1}{Nk_{\mathrm{B}}T^2}\left(\langle U^2\rangle_{NVT} - \langle U\rangle_{NVT}^2\right). \quad (15)$$

The isobaric heat capacity corresponds to a fluctuation formula in the NpT ensemble:

$$C_p = \frac{1}{Nk_{\mathrm{B}}T^2}\left(\langle H^2\rangle_{NpT} - \langle H\rangle_{NpT}^2\right). \quad (16)$$

5. Computational details

To introduce realistic polydispersity into our calculations we started from the experimental magnetization curves of ferrofluids [4]. The particle polydispersity is described by the gamma distribution

$$p(\xi) = \frac{\xi^\alpha \exp(-\xi)}{\Gamma(\alpha + 1)}, \quad (17)$$

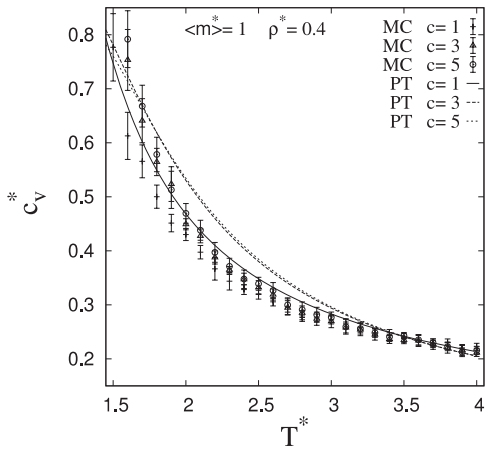

Figure 1. Temperature dependence of isochoric heat capacities of monodisperse and polydisperse magnetic fluids at the reduced density $\rho^* = 0.4$. The symbols represent the NVT ensemble MC simulation data while the lines represent the PT results.

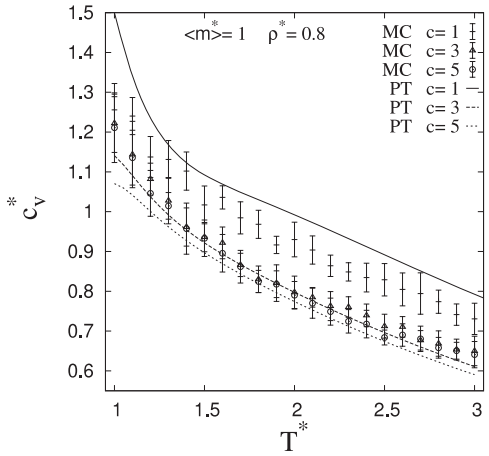

Figure 2. Temperature dependence of the isochoric heat capacities of monodisperse and polydisperse magnetic fluids at the reduced density $\rho^* = 0.8$. The symbols represent the NVT ensemble MC simulation data while the lines represent the PT results.

where $\xi = \sigma/\sigma_0$ is the relative diameter of particles, α is the parameter of the distribution, and Γ denotes the gamma function. Assuming spherical particles, the magnetic moment of a particle m_i depends linearly on the bulk magnetization of the ferromagnetic component M_b:

$$m_i = M_\mathrm{b}\frac{\pi}{6}\sigma_i^3. \tag{18}$$

To model polydispersity of the magnetic interactions we assumed that this relation is valid for each individual particle of the ferrofluid, i.e., $m_i \propto \sigma_i^3$. In this work the heat capacities of polydisperse ferrofluids are approximated by the corresponding properties of one-, three-, and five-component dipolar mixtures. The discretization of the distribution function is performed in such a way that the relative deviation in $\langle\sigma\rangle$ is less than 1.2%. The results for the dipolar (magnetic) fluids are presented in reduced units: $T^* = k_\mathrm{B}T/\epsilon$ is the reduced temperature, $\rho^* = \rho\langle\sigma^3\rangle$ is the reduced density with $\langle\sigma^3\rangle = \sum_i x_i\sigma_i^3$, $m^* = m/\sqrt{\epsilon\langle\sigma^3\rangle}$ is the reduced dipole moment, $p^* = p\langle\sigma^3\rangle/\epsilon$ is the reduced pressure, $c_V^* = C_V^\mathrm{c}/Nk_\mathrm{B}$ is the reduced configurational isochoric heat capacity, and $c_p^* = C_p^\mathrm{c}/Nk_\mathrm{B}$ is the reduced configurational isobaric heat capacity. In our calculations the one-component (monodisperse) fluid is characterized by uniform σ and m with the additional specification that $m^* = 1$. This value was assigned to the mean dipole moment of the polydisperse system ($\langle m^*\rangle = \sum_i x_i m_i^* = 1$) for the sake of comparison.

All NVT and NpT MC simulations were performed with either 343 or 512 particles. Boltzmann sampling and minimum image boundary conditions with half-cell cut-off and long-range corrections (LRCs) were used in both ensembles. For the dispersion part of the potential, the usual LJ-tail LRC was used, while for the dipole–dipole interaction a reaction field LRC with the conducting boundary condition was used. In the case of NVT simulations the number of cycles was between 1×10^5 and 2×10^5, while in the case of NpT simulations it was between 4×10^5 and 5×10^5 depending on the state point. The NVT starting configuration was a hcp lattice; the equilibration period was $2\times10^4-4\times10^4$ cycles. The NpT runs were started from the equilibrated NVT configurations. The statistical errors were calculated on the basis of the standard deviations of 10 subaverages.

6. Results and discussion

Preliminary phase equilibrium computations have been performed to establish state points for the heat capacity calculations that are outside the two-phase regions. (For one-component systems see [13] and [14].) At constant volume, we have chosen the reduced densities $\rho^* = 0.4$ and 0.8 that correspond to dilute and dense liquid phase points, respectively, in the temperature range studied. At constant pressure, two supercritical pressure values have been chosen ($p^* = 0.5$ and 1). Calculations using the conformal solution theory [12] to rescale the mixture integrals into one-component ones showed that in the case of lower temperatures the PT overestimates the simulation data by 50–70% for both three- and five-component mixtures. Obviously, cross correlations important at low temperatures are neglected in this approach; therefore, we did not pursue this route. In this work, the mixture integrals were scaled by the van der Waals one-fluid theory given by equations (9) and (10). Figure 1 shows the isochoric heat capacities for $\rho^* = 0.4$ as a function of the temperature. For both the monodisperse and polydisperse magnetic fluids c_V^* decreases with increasing temperature. Both methods show that the polydispersity causes only a small increase in c_V^*. This increase is larger at lower temperatures where correlations between species of different size and the dipole have a more significant effect, while at higher temperatures these correlations are reduced by thermal motion. The agreement between MC and PT is also better at high temperatures.

At the higher density $\rho^* = 0.8$, a considerable decrease in the heat capacity appears as polydispersity is turned on (figure 2). Interestingly, using a five-component mixture does

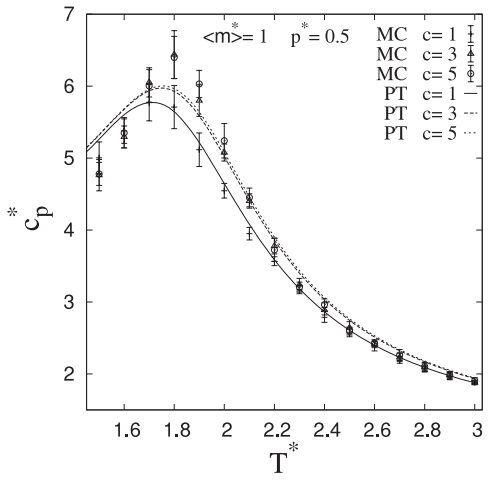

Figure 3. Temperature dependence of isobaric heat capacities of monodisperse and polydisperse magnetic fluids at the reduced pressure $p^* = 0.5$. The symbols represent the NpT ensemble MC simulation data while the lines represent the PT results.

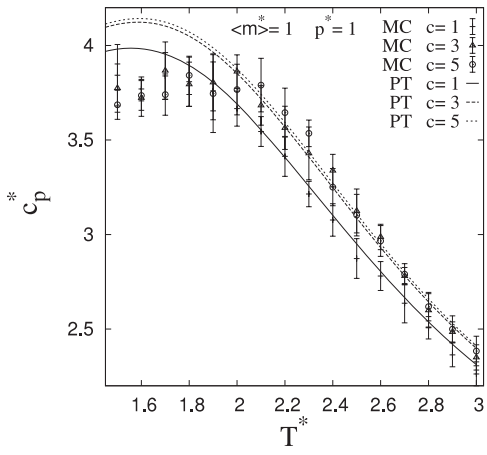

Figure 4. Temperature dependence of isobaric heat capacities of monodisperse and polydisperse magnetic fluids at the reduced pressure $p^* = 1$. The symbols represent the NpT ensemble MC simulation data while the lines represent the PT results.

not change the results significantly compared to the three-component case as shown by both simulation and theory. The agreement between MC and PT is better than in the previous case. This is not surprising because at higher densities the fluid structure is not so strongly perturbed by the addition of dipolar forces; the dominant effect is given by the short-range forces [9]. The effect of polydispersity is not so sensitive to the temperature as in the case of the dilute system: the shift appears at high temperatures too. The temperature dependences of the isobaric heat capacities are displayed in figures 3 and 4 for a lower ($p^* = 0.5$) and a higher ($p^* = 1$) pressure, respectively. The polydispersity causes some increase in the isobaric heat capacity. As in the case of c_V^* at high density (figure 2), the results for $c = 3$ and 5 are very close to each other. Also, in accordance with the results for c_V^*, the increase in the heat capacity is smaller at high temperatures when the system is more diluted. The lower pressure in figure 3 corresponds to lower densities in the range of $\rho^* = 0.16$–0.66 as opposed to the density range $\rho^* = 0.30$–0.74 in the case of figure 4.

The pronounced maxima at the reduced temperature $T^* \simeq 1.75$ are a fingerprint of a liquid–vapor-like phase transition, which takes place at lower pressures. For the critical pressure, the c_p^* versus T^* curves diverge at the critical temperature. Increasing the pressure, this divergence becomes a maximum as was shown for the LJ fluid before [6]. At higher pressures, the maximum is less pronounced as shown by figure 4. The agreement between the simulation data and the theoretical calculations is quantitatively good. Note that we have performed MC simulations for seven-component mixtures as well, but within the uncertainty of the simulation data we have not found any difference between the heat capacity data for the five- and seven-component mixtures. This means that a five-component mixture approximation is enough for calculating the heat capacities of polydisperse magnetic fluids assuming that the fluid does not have an extreme polydispersity. The theoretical calculations also confirm this conclusion.

From a theoretical point of view it is possible to work with continuous polydispersities as well. In that case, the summations in equations (6), (7) and (11) have to be substituted with integrations, while the number concentrations have to be substituted with the probability density function of equation (17). However, the corresponding integrals can be calculated only numerically. Work in this direction is in progress [15].

7. Summary

The isochoric and isobaric heat capacities of monodisperse and polydisperse ferrofluids have been calculated at different densities and pressures using NVT and NpT MC simulation methods. It has been found that at high densities the isochoric heat capacity decreases with increasing polydispersity, while the isobaric heat capacity increases with increasing polydispersity. A PT method has been proposed for calculating the heat capacities of monodisperse and polydisperse ferrofluids. Reasonable quantitative agreement has been found between the theoretical and simulation results.

Acknowledgments

The authors would like to thank the Hungarian Scientific Research Fund (Grant No. OTKA K61314) for financial support. We thank D Boda (Rush University, Chicago) for helpful correspondence.

References

[1] Ivanov A O 1999 *J. Magn. Magn. Mater.* **201** 234
[2] Kristóf T, Liszi J and Szalai I 2004 *Phys. Rev.* E **69** 062106
[3] Kristóf T and Szalai I 2003 *Phys. Rev.* E **68** 041109
[4] Ivanov A O, Kantorovich S S, Reznikov N, Holm C, Pshenichnikov A F, Lebedev V, Chremos A and Camp P J 2007 *Phys. Rev.* E **75** 061405
[5] Kristóf T and Szalai I 2005 *Phys. Rev.* E **71** 031109
[6] Boda D, Lukács T, Liszi J and Szalai I 1996 *Fluid Phase Equilib.* **119** 1

[7] Kronome G, Kristóf T, Liszi J and Szalai I 1999 *Fluid Phase Equilib.* **155** 157
[8] Józefczak A, Skumiel A and Labowski M 2005 *J. Magn. Magn. Mater.* **290/291** 265
[9] Gray C G and Gubbins K E 1984 *Theory of Molecular Fluids* vol 1 *Fundamentals* (Oxford: Clarendon)
[10] Johnson J K, Zollweg A and Gubbins K E 1993 *Mol. Phys.* **78** 591
[11] Luckas M, Luckas K, Deiters U and Gubbins K E 1986 *Mol. Phys.* **57** 241
[12] Two C H, Gubbins K E and Gray C G 1976 *J. Chem. Phys.* **64** 5186
[13] Smit B, Williams C P, Hendriks E M and De Leeuw S W 1989 *Mol. Phys.* **68** 765
[14] Stevens M J and Grest G S 1995 *Phys. Rev.* E **51** 5976
[15] Szalai I and Máté Z 2007 to be published